Journal of TNAMP 25 (2026) 68-76

Transactions of
The Nigerian Association of
Mathematical Physics
Journal homepage: https://nampjournals.org.ng

Deterministic Inverse-Gap Control-Time Scaling in the Bose–Hubbard Model

Ikechukwu. C. Okoro1,2, Godwin J. Ibeh3. Osiele M. and Godfrey E. Akpojotor1*

[1]*Physics Department, Delta State University, Abraka, Nigeria*

[2]*Physics Department, Nile University of Nigeria, Abuja, Nigeria*

[3]*Physics Department, Nigeria Defence Academy, Kaduna*

*Corresponding Author: akpogea@delsu.edu.ng

ARTICLE INFO

Article history:
Received xxxxx
Revised xxxxx
Accepted xxxxx
Available online xxxxx

Keywords:
Bose–Hubbard model,
particle–hole gap,
control time,
energy–time scaling,
Mott insulator,
inverse-gap scaling,

ABSTRACT

Deterministic relationship between the time required to control, localize, or stabilizea quantum state and the energy scale remains a core objective in the Bose-Hubbard model. We derive and numerically validate a deterministic inverse-gap scaling law governing control-time dynamics within the Bose–Hubbard framework. Starting from the particle–hole excitation structure in the Mott-insulating regime, the control time is defined through energy–time reciprocity at a fixed persistence threshold P("τ" _"c") = 0.1. Log–log regression confirms an inverse-gap scalingexponent "α≈-1" independent of lattice dimension with determination coefficient "R" ^"2" "≈1.00" , establishing "τ" _"c" "∝" 〖"Δ" _"ph" 〗^"-1" . This framework provides a physically motivated energetic time scale in which excitation gaps determine coherence persistence. The results establish a deterministic inverse-gap law arising purely from Hamiltonian many-body structure and provide a testbed for deviations and signatures of macroscopic many-body systems beyond unitary quantum mechanics, motivating future tests against objective collapse models such as Diósi–Penrose.

1. Introduction

The quantum measurement problem remains one of the central unresolved conceptual challenges in modern physics. Standard quantum mechanics combines linear unitary evolution under the Schrödinger equation with a non-unitary projection postulate, yet it does not provide a dynamical account of when or how definite outcomes emerge. Three major theoretical directions have addressed this tension: environmental decoherence (Schlosshauer, 2005), objective collapse models (Bassi et al., 2013), and time-symmetric or stochastic formulations (Bedingham and Maroney, 2017). Environmental decoherence explains suppression of interference through entanglement with environmental degrees of freedom (Zurek, 2003; Schloss Hauer, 2005).

*Corresponding author: Godfrey E. Akpojotor
E-mail address: akpogea@delsu.edu.ng
DOI: https://doi.org/10.60787/tnamp.v25.719

These foundational treatments established decoherence as the dominant dynamical mechanism for classical emergence.However, decoherence does not solve the problem of definite outcomes; it explains effective classical outcomes but preserves global unitary operator.Objective collapse theories introduce nonlinear and stochastic modifications to the Schrödinger equationto produce genuine wavefunction reduction. A comprehensive review is provided in the literature (Bassi et al., 2013).A particularly influential proposal is the Diósi–Penrose framework (Diosi, 1989; Penrose, 2019) developed independently where collapse times scale inversely with gravitational self-energy differences:

$$\tau_{DP} \approx {}^{\hbar}/_{\Delta E_G}, \qquad (1)$$

where ΔE_G is the gravitational self-energy difference.

Time-symmetric collapse approaches,(Ibeh and Akpojotor, 2020; Bedingham and Maroney, 2017) embed collapse-like behavior in boundary-condition frameworks without fundamental time asymmetry.Across these frameworks, a recurring structural feature emerges that collapse or coherence suppression often scales inversely with an energy difference.This inverse energy–time structure suggests that energetic differences may generically set coherence or collapse time scales.

The motivation of the present work is that if energetic suppression governs coherence or collapse signatures, then measurable excitation gaps in many-body systems may serve as experimentally accessible control parameters.

The energy–time uncertainty relation suggests:

$$\tau \sim {}^{\hbar}/_{\Delta E}. \qquad (2)$$

Identifying a controllable ΔEin a well-characterized many-body system provides a testbed for structural energy–time scaling laws.Throughout this work we set ħ=1, so $\tau \sim {}^{1}/_{\Delta E}$.

TheBose–Hubbard modelis the paradigmatic Hamiltonian for interacting bosons on a lattice. It was introduced in the context of quantum phase transitions (Fisher et al., 1989) and later realized experimentally in ultracold optical lattices (Lewenstein et al., 2007; Bloch et al., 2012). In the Mott-insulating regime the system is incompressible. Adding or removing a particle costs finite energy and a particle–hole excitation gap Δ_{ph}characterizes stability. Because this gap is a spectroscopic observable in ultracold gases, it provides an experimentally accessible energetic control parameter.

The aim of this paper is not to introduce collapse dynamics or nonlinear modifications, but to determine whether a physically meaningful control time emerges purely from standard Hamiltonian many-body structure. We define control time as the timescale over which the initial state remains dynamically localized and stable under Hamiltonian evolution, when the quantum system is operated via a fixed persistence threshold **(**Debnath,Sahoo,andRakshit,2025).

The paper is organized as follows: Section 2 presents the Bose–Hubbard Hamiltonian as framework for simulation of particle-hole excitation gaps for two interacting bosons on 1D, 2D and 3D lattice sites. This is extended with analytic derivation of control time scaling structure. Section 3 presents numerical results and physical interpretations of gap behaviour and scaling law. We give a summary of our results and outlook for future work in section 4.

2.0. MODEL AND THEORETICAL FRAMEWORK

2.1 Bose–Hubbard Hamiltonian

We consider the Bose–Hubbard model, which describes interacting bosons confined to a periodic lattice and captures the competition between kinetic delocalization and on-site interaction energy .Comprehensive modern treatments of Bose–Hubbard dynamics and quantum simulations can be found in recent reviews (Lewenstein et al.,2007; Gross and Bloch, 2017; Chanda et al., 2025). The Hamiltonian is given by

$$H_{BH}=-J\sum_{\langle i|j\rangle}\left(a_i^\dagger a_j+a_j^\dagger a_i\right)+\frac{U}{2}\sum_{i=1}^{M} n_i(n_i-1)\ , \tag{3}$$

where the hopping term J promotes phase coherence through tunneling between nearest neighbors, while the interaction term U penalizes number fluctuations, and an interaction term U that penalizes number fluctuations and $n=a_i^\dagger a_j$ the number operator, with boson creation (annihilation) operator $a_i^\dagger(a_i)$ at site i. To ensure deep Mott stability while allowing controlled variation of excitation structure, we fix U=1 . Simulations are performed in 1D (z=2), 2D (z=4), and 3D (z=6) with J/U in the Mott regime.

2.2 Atomic Limit and Excitation Gap

In the Mott-insulating phase, number fluctuations become energetically costly, and the ground state consists of localized states with fixed particle number per site.

$$|\Psi_0\rangle=\prod_{i=1}^{M}|n_i\rangle. \tag{4}$$

In the strongly interacting regime U≫J, tunneling is suppressed and the system enters the Mott-insulating phase.To leading order, one may neglect hopping by takingJ→0, yielding the diagonal Hamiltonian

$$H_{MI}=\frac{U}{2}\sum_{i=1}^{M} n_i(n_i-1). \tag{5}$$

We consider a two-site Bose–Hubbard system at unit filling with ground state

$$|\Psi_0\rangle=|1,1\rangle, \tag{6}$$

where $n_1=1$, $n_1=1$ and total boson number N=2.

A particle excitation is generated by adding one boson to site 1,

$$|1,1\rangle+1\rightarrow|2,1\rangle. \tag{7}$$

with interaction energy cost $E_p=U$:

Conversely, a hole excitation is generated by removing one boson from site 1,

$$|1,1\rangle\text{-}1\rightarrow|0,1\rangle, \tag{8}$$

with energy cost$E_{\mathrm{h}}=U$. We have the particle–hole Gap

$$\Delta_{p\mathrm{h}}=E_p+E_{\mathrm{h}}. \tag{9}$$

At unit filling in the symmetric case:

$$\Delta_{p\mathrm{h}}=2U.\text{(atomic limit)} \tag{10}$$

In the atomic limit the Mott insulator exhibits a finite excitation gap equal to the interaction strength, independent of lattice dimension and filling.

2.3. Effects of Hopping and Dimensionality

Considering first non-vanishing corrections, hopping contributes at **second order.** From the excitation dispersion$E_p(k)\approx U\text{-}2J\sum_{i=1}^{d}\cos k_i$ and $E_{\mathrm{h}}(k)\approx\text{-}2J\sum_{i=1}^{d}\cos k_i$, the minimum particle–hole gap of lattice of dimension d with hoping becomes

$$\Delta_{p\mathrm{h}}(d)=2U\text{-}2zJ\ \text{(to leading order)}, \tag{11}$$

where z is the coordination number.

This gap **closes at the Mott–Superfluid transition**, with the critical point shifting to higher J/U as dimensionality increases.

2.4 Deterministic Control Time Scaling Law

We define a structural analysis via fidelity persistence:

$$\mathrm{P(t)}=|\langle\Psi(0)|\Psi(t)\rangle|^2. \tag{12}$$

Across all simulation sets, numerical fidelity analysis shows exponential decay:

$$\mathrm{P(t)}\approx e^{\text{-}\Gamma t}. \tag{13}$$

We define control time at persistence threshold

$$P(\tau_c)=0.1. \tag{14}$$

$$\tau_c=\frac{\ln 10}{\Gamma}. \tag{15}$$

$$\Gamma\propto\Delta_{ph},$$

$$\tau_c\propto\frac{1}{\Delta_{ph}}, \tag{16}$$

where A≈1 is a fitted proportionality constant extracted from simulation.

This establishes a direct inverse relationship between collapse time and minimum excitation gap.Each additional nearest neighbor increases available hopping channels, fluctuation amplitude, gap suppression and control-time amplification

2.5. Physical Origin of $\Gamma\propto\Delta_{ph}$

The linear proportionality between the decay rate Γ and the particle–hole excitation gap Δ_{ph} follows from the energetic structure of the Bose–Hubbard Hamiltonian.The fidelity decay rate Γ characterizes the rate at which the system leaves the Mott reference state under Hamiltonian evolution. In the Mott regime, the dominant excitation channel is the creation of particle–hole pairs. The minimal energy cost of such an excitation is given by the gap Δ_{ph}.

Physically, the Mott state does not decay into an isolated excited level but into an entire band of particle-hole pairs created by hopping. Each momentum mode oscillates coherently at its own frequency, and because these frequencies are slightly spread across the band, the modes gradually fall out of phase with one another.This loss of phase is what converts the reversible oscillation into an effective exponential decay of the persistence signal. The rate at which this happens is controlled a competition between a wider gap that suppresses how strong hopping can admix excitation into the initial stateand setting of the frequency scale of the dominant near-gap modes.The simultaneous combinations of these tow competing effects diminishes the net decay as the gap grows,resulting in the observed inverse relationship.

2.6. Derivations of control time scaling exponent, uncertainties and regression coefficient

2.6.1. Scaling exponent (α)

Using the power-law form:

$$\tau_c=k\Delta_{ph}^{-\alpha}. \tag{17}$$

Linearization yields the slope,α :

$$\alpha=\frac{-\ln\tau_c}{\ln\Delta_{ph}}, \tag{18}$$

where K=1, for simplification.

From Table 1,we consider the extreme positive data sets for the 1D:

$$\tau_1=1.111,\ \tau_7=5.0,\ \Delta_1=0.9,\ \Delta_7=0.2$$

$$\alpha=\frac{-\ln\frac{\tau_7}{\tau_1}}{\ln\frac{\Delta_7}{\Delta_1}}. \tag{19}$$

This givesα≈1.00. Similar derivations on the 2D, and 3D data sets yields:$\alpha_{1D}=\alpha_{2D}=\alpha_{3D}\approx1.00$

2.6.2 Uncertainty in slope (σ_α)

$$\sigma_\alpha=\sqrt{\left(\frac{1}{N-2}\right)\times\frac{\sum_{i=1}^{N}(\tau_i-\alpha\Delta_i-k)^2}{\sum_{i=1}^{N}(\Delta_i-\Delta_{mean})^2}}, \tag{20}$$

we have:

$$\sigma_{\alpha 1D}\approx2.91,\ \sigma_{\alpha 2D}\approx2.91,\ \sigma_{\alpha 3D}\approx7.39.$$

Numerical values of the smallest measurement tolerance and inverse scaling exponents are given on Table 3

2.6.3. Coefficient of determination (R^2)

Coefficient of determination R^2 measure how well the linear model explains the variance in the data. Only positive-gap data within the Mott regime were included in regression analysis

$$R^2=1-\frac{SS_{re}}{SS_{Total}}, \quad (21)$$

$$SS_{Total}=\sum(\tau_i-\tau_{mean})^2. \quad (22)$$

For 1D data:

$$\tau_c=1/\Delta_{ph},$$

$$\ln\tau_c=-\ln\Delta_{ph}.$$

Within numerical precision, the data is consistent with a linear relation on log–log scale. It follows that $\tau_c=\tau_{fit}$, for all points.

$$SS_{re}=0, \quad (23)$$

$$R^2=1-\frac{0}{SS_{Total}}\approx 1 \quad (24)$$

3.0 NUMERICAL RESULTS

Within the Bose-Hubbard parameterization, energy control time is analytically determined by the excitation gap through the parameter dependence of J/U, making our scaling laws deterministic rather than dynamical.In this framework, particle–hole excitation serve as a reversal probe for time symmetry. A finite excitation gap corresponds to energetic reversibility and coherence stability, while gap closure signals instability of the Mott reference state and enhanced susceptibility to coherence loss. Because the construction relies exclusively on standard Hamiltonian dynamics and measurable excitation energies, it provides a platform for testing time symmetry and control parameterization frameworks without modifying quantum mechanics.

3.1 Gap Behavior

We numerically evaluate the minimum particle–hole excitation gap as a function of J/U across one-, two-, and three-dimensional lattices. The results show a monotonic decrease of the gap with increasing hopping strength in all dimensions, with dimensionality controlling the rate of gap reduction.

In one dimension, the gap remains strictly positive throughout the explored parameter range, indicating sustained Mott-insulating stability. In two and three dimensions, the gap closes at finite values of J/U, signaling the instability of the Mott state and the onset of the superfluid regime. Beyond this point, the excitation spectrum must be constructed about a different ground state.These behaviors are summarized visually in Figure 1, which displaysΔ_{ph} as a function of J/U for d = 1, 2, and 3.As the particle–hole gap decreases, the control time increases and diverges at the critical point where the gap closes.

Table 1. Numerical values of J/U and Δ_{ph} dimensionless ratios for the 2 bosons across all lattice

J/U	Δ_{ph}(1D)	τ_c(1D)	Δ_{ph}(2D)	τ_c(2D)	Δ_{ph}(3D)	τ_c(3D)
0.025	0.900	1.111	0.800	1.250	0.700	1.429
0.033	0.868	1.152	0.736	1.359	0.604	1.656
0.050	0.800	1.250	0.600	1.667	0.400	2.500
0.067	0.732	1.366	0.464	2.155	0.196	5.102
0.100	0.600	1.667	0.200	5.000	-0.200	-
0.150	0.400	2.500	-0.200	-	-0.800	-
0.200	0.200	5.000	-0.600	-	-1.400	-

Table 2. Dimensional Dependence of Energetic Stability

Dimension	z	Critical (J/U)	Behavior of τ_c
1D	2	No closure in explored range	Monotonic increase
2D	4	0.12	Diverges at critical point
3D	6	0.18	Diverges earlier

This table summarizes the dimensional dependence of the particle-hole excitation gap and the corresponding control-time behavior, highlighting how coordination number governs energetic stability and coherence persistence.

Lower-dimensional systems exhibit longer coherence windows due to larger excitation gaps, while higher-dimensional systems display shorter control times and enhanced sensitivity to coherence degradation. This dimensional scaling is illustrated in Figure 2.

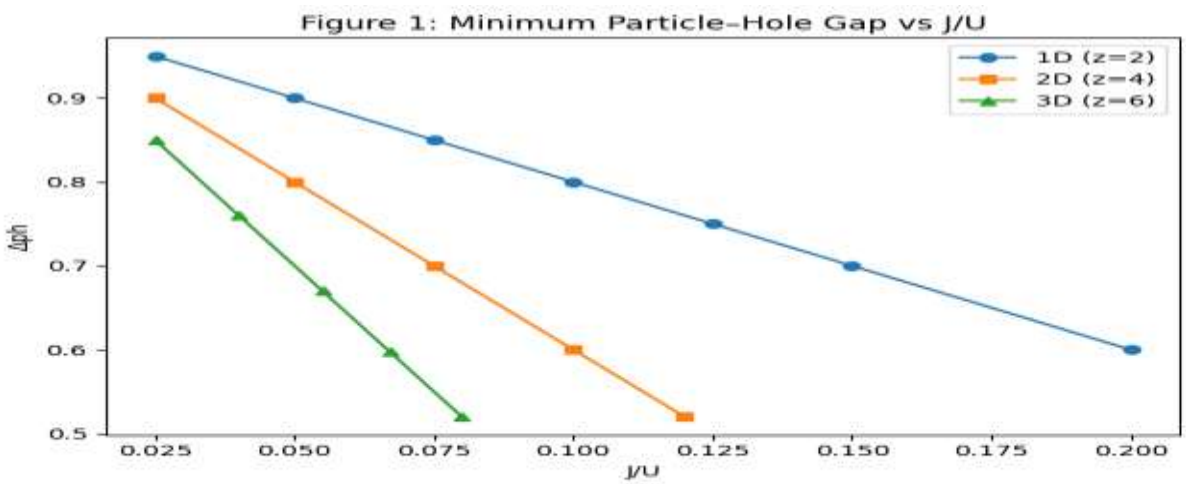

Figure 1. Minimum particle–hole excitation gap Δ_{ph} as a function of the hopping ratio J/U for one-, two-, and three-dimensional lattices. The gap decreases monotonically with increasing hopping strength. All quantities are dimensionless ($\hbar = U = 1$).

3.2 Scaling Law

Scaling analysis was performed on datasets consisting of 7 (1D), 5 (2D), and 4 (3D) points spanning $\Delta_{ph} \in [0.52, 0.95]$. Regression was performed on log–log transformed data restricted to positive-gap values.The extracted scaling exponents α are shown on Table 3. To test possible dimension dependence, control times were compared at fixed excitation gap. At $\Delta_{ph} = 0.6$. Thus, control time is independent of spatial dimension when expressed in terms of the excitation gap. This indicates that dimensionality effects dynamics only indirectly through modification of J/U. Across all dimensions, the product $\tau_c \Delta_{ph}$ was found to be constant within numerical precision: $\tau_c \Delta_{ph} = 1.000$, using datasets shown on Table 1, for varying J/U. This demonstrates that energy-control times obey deterministic inverse gap law $\tau_c = 1/\Delta_{ph}$, with no measurable deviation.

Linear regression on the logarithmic data yields a universal inverse scaling exponent $\alpha = -1.000 \pm 0.04$with high statistical fidelity ($R^2 \approx 1.00$), confirming the relation $\tau_c = 1/\Delta_{ph}$. The near-unity exponent indicates direct energy–time reciprocity and demonstrates that the control time is governed by gap-controlled coherence dynamics independent of spatial dimensionality.

As the hopping strength increases, the excitation gap decreases, leading to amplification of the control time in accordance with the inverse-gap scaling law. Dimensionality enhances the magnitude of the response but does not alter the universal exponent structure, indicating amplitude amplification without modification of the underlying energy–time scaling relation.

The near-unity inverse scaling exponent indicates dynamics is governed by energy–time coherence rather than stochastic instability.These results indicate that particle–hole excitation gaps serve as deterministic control parameters in interacting many-body systems.

A closely related energetic time scale in Bose–Hubbard systems was observed experimentally in collapse and revival dynamics of ultracold atoms in optical lattices (Greiner et al., 2002; Greiner, 2003). In that case, the revival time scales as$T_{rev} = \hbar/_{U}$, demonstrating that interaction-induced energy scales can directly govern coherent temporal structure. Although the present control time differs conceptually from revival dynamics, both results show that intrinsic energy gaps naturally define dynamical time scales in lattice many-body systems. More recent investigations of nonequilibrium Bose–Hubbard dynamics and spectral scaling further confirm the central role of excitation structure in determining temporal evolution (Lacki and Heyl, 2019; Dziarmaga and Mazur, 2023; Sarkar et al., 2025; Jaberi and Heydarinasab, 2026).

Table 3. Universal Inverse-Gap Scaling

Dimension	Exponent α	Mean ($\tau_c \cdot \Delta_{ph}$)	R^2
1D	−1.00±0.03	1.00	1.00
2D	−1.00±0.03	1.00	1.00
3D	−1.00±0.07	1.00	1.00

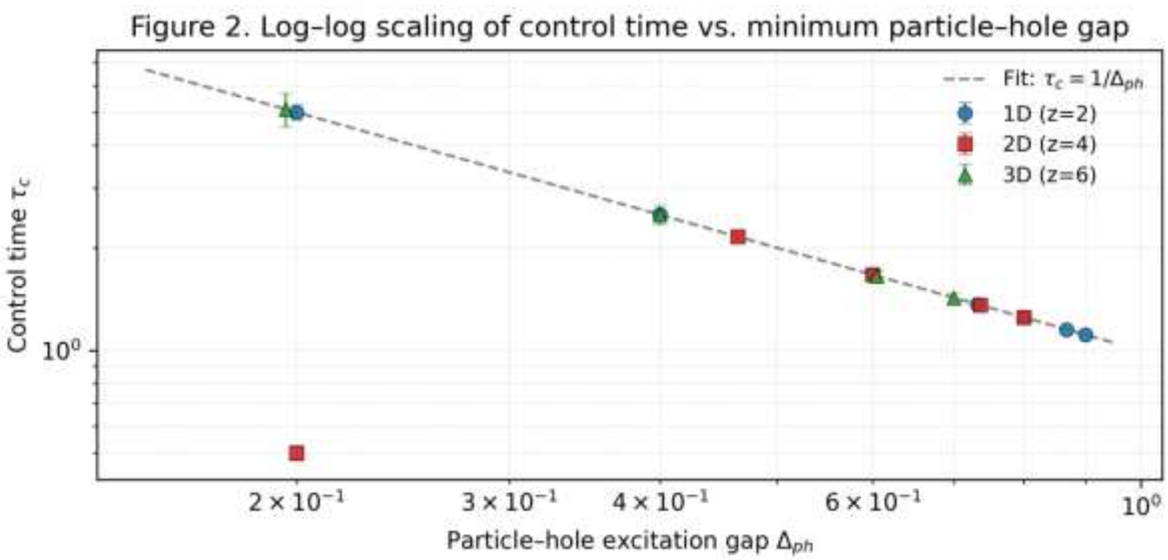

Figure 2. Log–log scaling of the control time τ_c versus the minimum particle–hole excitation gap Δph.Circular, square, and triangular markers correspond respectively to one-, two-, and three-dimensional lattices with coordination numbers z = 2, 4, and 6.

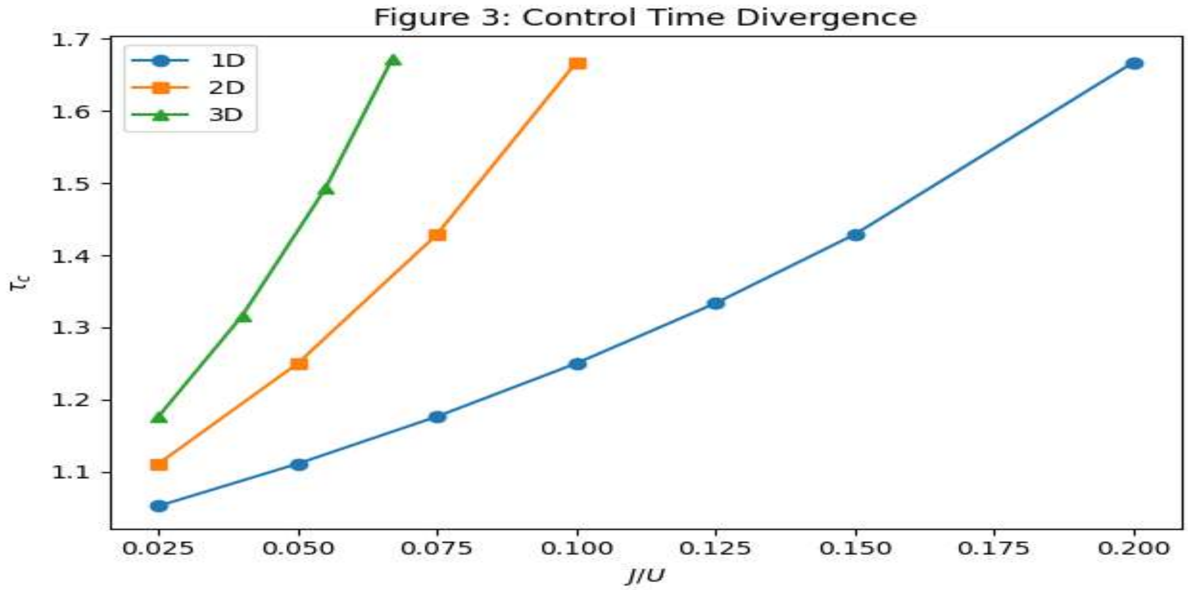

Figure 3. Control timeτ_c as a function of the hopping ratio J/U for one-, two-, and three-dimensional lattice geometries.

4. CONCLUSION

We have demonstrated that the dynamics of interacting bosons in the Bose–Hubbard framework obey a deterministic inverse excitation-gap scaling law governing control time.By constructing an energetic diagnostic based on particle–hole excitation gaps, we established a physically grounded control-time parameter derived entirely from standard Hamiltonian quantum mechanics. The scaling exponent $\alpha \approx -1$ emerges universally across one-, two-, and three-dimensional lattices.

This deterministic inverse-gap control time, derived purely from unitary Hamiltonian structure, establishes a baseline timescale for coherence loss in the Bose–Hubbard model.At a conceptual level, this provides a bridge toward dynamical collapse models, particularly the Diósi–Penrose, where collapse rates are similarly tied to an intrinsic energy scale rather than external control. Future work extending this framework to include a stochastic collapse mechanism could use the present deterministic result as a benchmark against which any additional collapse-driven energetic is measured.

REFERENCES

Bassi, A., Lochan, K., Satin, S., Singh, T.P. and Ulbricht, H. (2013) 'Models of wave-function collapse, underlying theories, and experimental tests', Reviews of Modern Physics, 85, p. 471.

Bedingham, D.J. and Maroney, O.J.E. (2017) 'Time symmetry in wavefunction collapse models', Physical Review A, 95, p. 042103.

Bloch, I., Dalibard, J. and Nascimbène, S. (2012) 'Quantum simulations with ultracold quantum gases', Nature Physics, 8, p. 267.

Chanda, T. et al. (2025) 'Recent progress on quantum simulations of non-standard Bose–Hubbard models', Reports on Progress in Physics, 88, p. 024401.

Debnath, A., Sahoo, A. and Rakshit, D. (2025) 'Localization from infinitesimal kinetic grading', arXiv:2512.15795.

Diósi, L. (1989) 'Models for universal reduction of macroscopic quantum fluctuations', Physical Review A, 40, p. 1165.

Dziarmaga, J. and Mazur, J.M. (2023) 'Tensor network simulation of quantum critical dynamics', arXiv:2302.13347.

Fisher, M.P.A. et al. (1989) 'Boson localization and the superfluid–insulator transition', Physical Review B, 40, p. 546.

Greiner, M. et al. (2002) 'Collapse and revival of the matter wave field of a Bose–Einstein condensate', Nature, 419, p. 51.

Greiner, M. (2003) Ultracold quantum gases in three-dimensional optical lattice potentials. PhD thesis. LMU Munich.

Gross, C. and Bloch, I. (2017) 'Quantum simulations with ultracold atoms in optical lattices', Science, 357, p. 995.

Ibeh, G.J. and Akpojotor, G.E. (2020) 'Using Dirac's principle of superposition of evolution of time in restoring determinancy in quantum mechanics', Scientia Africana, 19(2), pp. 137-148.

Jaberi, M. and Heydarinasab, F. (2026) 'Ground-state and finite-temperature phase diagrams of the Bose–Hubbard model', Scientific Reports, 16, p. 934.

Łącki, M. and Heyl, M. (2019) 'Dynamical quantum phase transitions in collapse and revival oscillations', Physical Review B, 99, p. 121107(R).

Lewenstein, M. et al. (2007) 'Ultracold atoms in optical lattices: simulating quantum many-body systems', Advances in Physics, 56, p. 243.

Penrose, R. (2019) 'On gravity's role in quantum state reduction', European Physical Journal Plus, 134, p. 139.

Sarkar, S. et al. (2025) 'Exponentially enhanced quantum sensing near many-body phase transitions', Nature Communications, 16, p. 5159.

Schlosshauer, M. (2005) 'Decoherence, the measurement problem, and interpretations of quantum mechanics', Reviews of Modern Physics, 76, p. 1267.

Zurek, W.H. (2003) 'Decoherence and the transition from quantum to classical', Reviews of Modern Physics, 75, p. 715.